RADIATION-RESISTANT FIBER OPTIC STRAIN SENSORS FOR SNS TARGET INSTRUMENTATION*

Yun Liu†, Willem Blokland, Jeff Bryan, Abdurahim Rakhman, Bernie Riemer, Robert Sangrey, Ryan Strum, Mark Wendel, Drew Winder
Spallation Neutron Source, Oak Ridge National Laboratory, Oak Ridge, TN 37831, USA

Abstract

Measurement of stresses and strains in the mercury target vessel of the Spallation Neutron Source (SNS) is important to understand the structural dynamics of the target. This work reports the development of radiation-resistant fiber optic strain sensors for the SNS target instrumentation. Experimental results demonstrated the suitability of the sensor for measurement of ~ 100 kHz strains at up to 10^9 Gy radiation doses.

INTRODUCTION

The Spallation Neutron Source (SNS) target modules are stainless steel vessels through which mercury target material is pumped. The target is struck by 1 GeV, up to 24 μC pulses of protons at 60 Hz to produce the world most powerful neutrons for science applications. Establishing the capability to measure the stresses and strains in the mercury vessel is important to understand the structural dynamics of the targets and also a pre-requisite to assessing the success of gas injection to mitigate pressure-pulse loads on the target vessel [1].

Owing to their compactness, easy system integration, and invulnerability to the electromagnetic interference, fiber optic strain sensors have been actively employed to directly measure the strain on the target vessel. In 2015, commercial fiber-optic strain sensors were installed on the SNS target 13. The sensors were mounted directly on the target mercury vessel in the interstitial space between the mercury vessel and the outer water-cooled shroud. While the sensors did serve their function and strain data for anticipated time period have been recorded, due to radiation induced damage, the sensor only lasted a few hundred pulses and stopped functioning before the target was switched to the neutron production mode.

In this paper, we report the development of radiation-resistant fiber optic strain sensors. The sensor uses a Fluorine-doped single-mode SiO_2 fiber which shows a strong radiation-resistance at the 1300 nm wavelength range. A low-coherence interferometer is used in the sensor to obtain a high signal-to-noise ratio. The sensor output is processed with a Fizeau interferometer as the local reference interferometer (LRI). A phase shifting detection scheme is used to accurately track the strain change. The measurement is conducted at MHz sampling rates and 200 kHz bandwidth. Experimental results demonstrated the suitability of the sensor for study of the SNS target at the neutron production proton beam.

* Work supported by U.S. Department of Energy under contract DE-AC05-00OR22725.
† liuy2@ornl.gov

MEASUREMENT OF RADIATION INDUCED ABSORPTION IN FIBER

The radiation-resistant fiber is a Fluorine-doped single-mode fiber (Fujikura RRSMFB) [2]. Both the core and cladding of the fiber are Fluorine doped SiO_2 with different Fluorine concentration ratios. It was found that such a doping can result in a higher radiation resistance in the long wavelength range as Fluorine decreases the glassy disorder and strains the Si-O bonds in silica. The OH concentration in the fiber core is minimized to optimize the transmission in long wavelength region. The fiber has a cladding diameter of 125 μm and core MFD of 8.7 μm at 1310 nm. The loss specification is about 0.38 dB/km at 1310 nm.

Previously, the radiation induced absorption (RIA) of the fiber was investigated using a Co source and in the Super proton Synchrotron at CERN. The fiber showed a quite low attenuation (< 5 dB/km) for light at 1310 nm after a total dose of 1 MGy at the maximum dose rate of a few Gys per second. However, the interstitial space of the SNS mercury target has a much higher dose rate and total dose amount.

The radiation test has been conducted by installing an open fiber loop inside the interstitial space of the target. About a 2-meter long fiber is attached on the surface of the steel mercury vessel using the Stycast epoxy. The location of the fiber loop in the coordinate of the target is measured so that the radiation level at each point can be estimated using the calculated energy deposition database. About 50 cm of the fiber loop is in the pre-calibrated radiation region that has the radiation doses ≥ 100 MRad/MWhr and, among which, about 10 cm of the fiber is located in a high radiation region that has the radiation doses > 1 Grad/MWhr. Here, MWhr indicates the energy of the proton beam delivered on the target.

A milli-watt level of the laser light at the wavelength of 1320 nm is sent into the fiber through two fiber relay cables with a total length of ~ 20 m. The radiation level outside the interstitial space of the target is many orders of magnitude lower than the interstitial space. Therefore we only count the radiation doses inside the radiation region with the radiation doses ≥ 100 MRad/MWhr. Figure 1 shows the measurement result of the fiber transmission during the first two weeks of the SNS target 13 commissioning. The data were taken in every 10 minutes. The transmission drops 3 dB at the energy on target level of 56.5 MWhr. The calculated RIA over the radiation region is equivalent to 0.4 dB/km/MRad while the RIA in the high radiation region is 0.9 dB/km/MRad. The peak

ISBN 978-3-95450-147-2

dose amount is 83.6 Grad and the peak dose rate is 329 kRad/s which occurs at the proton power of 800 kW. The result shows the strain sensor fabricated using the above radiation-resistant fiber can be used to measure the strains during the neutron production operation.

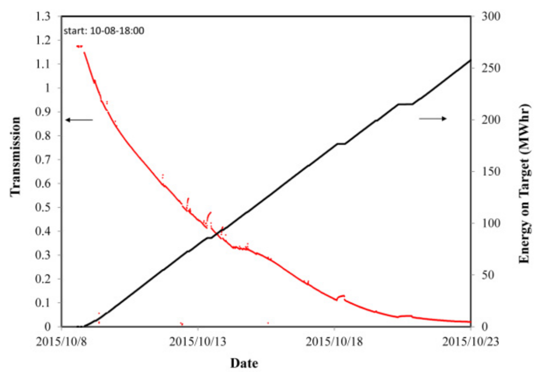

Figure 1: Optical power transmission of the fiber installed in the interstitial space of SNS target 13. Occasional spikes in the transmission curve indicate the temporary recoveries of the fiber transmission when the proton beam is turned off.

SENSOR SYSTEM

The fiber-optic strain sensor for the SNS target uses a low-coherence interferometer (LCI) configuration. The most important feature of the LCI is its insensitivity to the optical power fluctuations along the fiber link. This is particularly important in the case of SNS target instrumentation since there are uncontrollable optical power/polarization changes in the fiber caused by radiation, temperature variation, mercury flow and other factors. The light source used in the sensor is a fiber coupled superluminescent laser diode (model Thorlabs S5FC1018S SLD). The center wavelength of the SLD is 1.32 μm with the spectrum bandwidth of 36 nm. We measured the temporal coherence function of the light source using a Michelson interferometer which gives a coherence time $\tau_c \approx 0.1$ ps corresponding to a coherence length $l_c \approx 30$ μm. The sensor is a low-finesse Fabry-Perot cavity formed by the end surfaces of two fibers: the radiation-resistant single-mode fiber as a signal transmitting fiber and a commercial ϕ62.5 μm graded-index multimode fiber as a reflecting fiber. Both fibers are cleaved and attached inside a capillary tube with a gap distance between the fibers of ~ 65 μm. The sensor length is about 7 mm. To enhance the signal contrast, the reflecting surface of the multimode fiber is appropriately polished and coated with a thin Au film before the sensor assembly. The sensor was fabricated by LUNA Inc. A schematic of the optical setup is shown in Fig. 2.

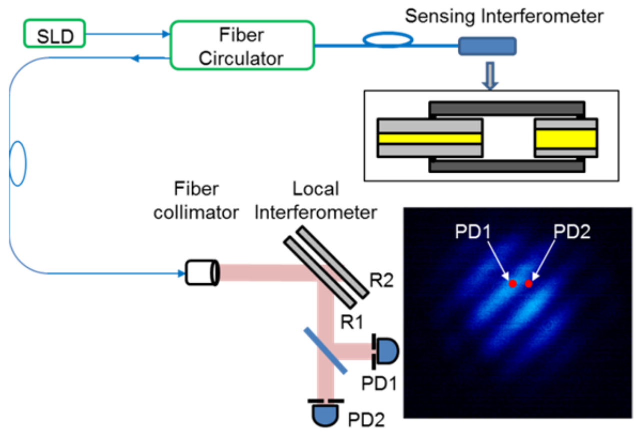

Figure 2: Optical setup of fiber-optic strain sensor using low-coherence interferometer. PD: photo-detector, R1, R2: reflectors. Inset boxes: Fabry-Perot cavity as the sensing interferometer (top) and interference fringes of the LRI output (bottom).

Since the optical path difference (OPD) of the sensing interferometer is 4 times longer than the coherence length of the light source, there is no direct interference between reflections from the two surfaces. The reflections from the sensing interferometer is coupled to a Fizeau interferometer based LRI for detection. When the OPD of the LRI is adjusted to match that of the sensing interferometer, within the coherence length of the light source, an interference will be observed in the output of the LRI. The phase of the resulting interference fringes will be a function of the difference between OPDs of the two interferometers.

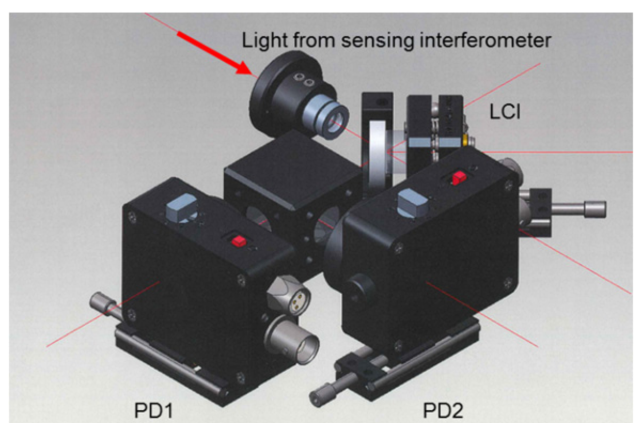

Figure 3: Layout of the local reference interferometer. Phase difference is set up by adjusting positions of PDs.

Conventional LCI technology [3] measures the absolute peak position of the interference fringes by modulating the OPD of the LRI. The sensing speed is largely restricted by the bandwidth of the scanning devices. Electronic scanning or channelled spectrum methods convert the temporal scan to a spatial pattern and therefore dramatically simplifies the detection process. However, the measurement speed is still limited by the bandwidth of the photo-detector arrays, such as CCDs. Those methods also suffer from low resolution and put a stringent requirement for the light source. On the other hand, the anticipated strains on the SNS mercury target are pulsed, fast and have relatively low magnitude (order of 100 με), a high speed and high resolution measurement is critical.

In this work, we propose a phase shifting detection approach to track the phase change of sensor output. As shown in the inset box of Fig. 3, the two detectors are properly located with a constant phase shift in the LRI output plane. By using phase shifted signals, the phase of the LRI output can be determined with no ambiguity. The phase difference is calibrated from the two detector output signals by scanning the LRI over a range larger than the wavelength prior to the measurement. The detector outputs are acquired using a commercial data acquisition electronics and phase tracking is performed in a computer. The measurement speed is only limited by the bandwidth of photo-detectors and digitizer. The present setup has a bandwidth of 200 kHz and sampling rates of up to 2 MHz.

MEASUREMENT PERFORMANCE

The strain measurement has been performed on a stainless steel test plate. Both the radiation-resistant sensor and a pre-calibrated commercial fiber optic strain sensor (FISO) are attached on the test plate. In one test, the plate is clamped at one end while the free end of the plate is slowly pressed or tapped. The press-release process will result in gradual strain on the sensor while a fast tapping causes damped oscillations at frequencies of 10 – 100 Hz. Figure 4 shows a typical example of the measurement results where the test plate was alternatively pressed and tapped. Obviously the two measurements match with each other very well.

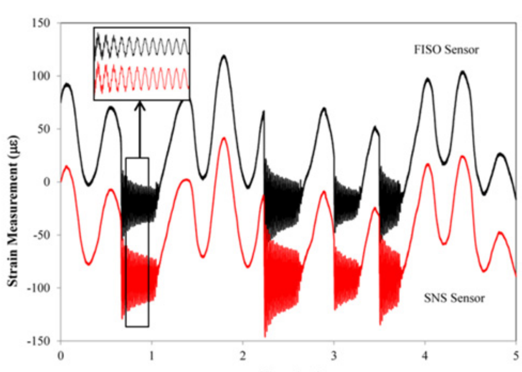

Figure 4: Measurement of strains created by push-release-tapping of the stainless steel test plate.

In the second test, both ends of the test plate were tightly clamped while a mechanical shock was applied to one point on the plate. Since different locations receive different strains in such a case, it is not easy to directly compare the measurement results from the two sensors. However, one can see the high frequency (KHz order) oscillations were seen at both sensors as shown in Fig. 5.

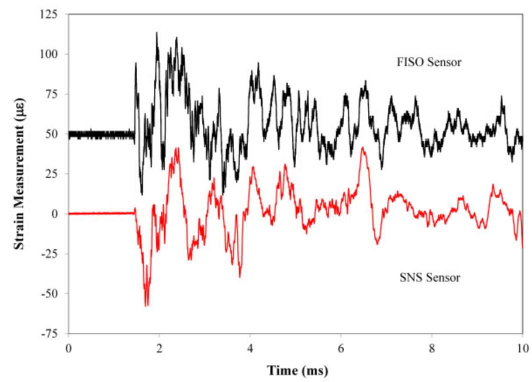

Figure 5: Measurement of high frequency strains created by applying a mechanical shock on the stainless steel test plate.

CONCLUSION

In conclusion, we have designed, implemented, and tested a fiber-optic strain sensor using a low-coherence interferometry and Fluorine-doped single-mode optical fiber. The radiation-induced absorption of the fiber has been measured in the interstitial space of the SNS mercury target at the neutron production proton beam (800 kW). The fiber shows about 0.9 dB/km loss at 1 MRad with the peak dose rate of 329 kRad/s. A Fabry-Perot type sensor has been fabricated using the radiation-resistant fiber and a Fizeau interferometer has been used as the local reference interferometer. A phase retrieve algorithm based on a phase shifting detection scheme has been developed to accurately recover the strain changes. We tested the sensor in comparison with a commercial strain sensor and a good agreement has been achieved. The sensor has been installed on the SNS target 14 and will be used to monitor the mercury vessel strains during neutron production.

ACKNOWLEDGMENT

We thank D. Hensley for the fiber coating, A. Menshov for the mechanical design, and J. Diamond for his help of assembly.

REFERENCES

[1] B.W. Riemer et al., “Small gas bubble experiment for mitigation of cavitation damage and pressure waves in short-pulse mercury spallation targets,” J. Nucl. Mater. 450 (2014) 192.

[2] K. Aikawa et al., “Radiation-resistant single-mode optical fibers,” Fujikura Technical Review (2008) 9.

[3] Y.J. Rao and D. A. Jackson, “Recent progress in fibre optic low-coherence interferometry,” Meas. Sci. Technol. 7 (1996) 981.

ISBN 978-3-95450-147-2